Adaptive Parameter Estimation and Control Design for Robot Manipulators With Finite-Time Convergence

Chenguang Yang, *Senior Member, IEEE*, Yiming Jiang, Wei He, *Senior Member, IEEE*, Jing Na, *Member, IEEE*, Zhijun Li, *Senior Member, IEEE*, and Bin Xu

***Abstract*—For parameter identifications of robot systems, most existing works have focused on the estimation veracity, but few works of literature are concerned with the convergence speed. In this paper, we developed a robot control/identification scheme to identify the unknown robot kinematic and dynamic parameters with enhanced convergence rate. Superior to the traditional methods, the information of parameter estimation error was properly integrated into the proposed identification algorithm, such that enhanced estimation performance was achieved. Besides, the Newton–Euler (NE) method was used to build the robot dynamic model, where a singular value decomposition-based model reduction method was designed to remedy the potential singularity problems of the NE regressor. Moreover, an interval excitation condition was employed to relax the requirement of persistent excitation condition for the kinematic estimation. By using the Lyapunov synthesis, explicit analysis of the convergence rate of the tracking errors and the estimated parameters were performed. Simulation studies were conducted to show the accurate and fast convergence of the proposed finite-time (FT) identification algorithm based on a 7-DOF arm of Baxter robot.**

Manuscript received September 1, 2017; revised November 20, 2017 and December 31, 2017; accepted January 19, 2018. Date of publication February 8, 2018; date of current version June 1, 2018. This work was supported in part by the National Nature Science Foundation under Grant 61473120 and Grant 61573174, in part by the Science and Technology Planning Project of Guangzhou under Grant 201607010006, in part by the State Key Laboratory of Robotics and System (HIT) under Grant SKLRS-2017-KF-13, in part by the Fundamental Research Funds for the Central Universities 2017ZD057, and in part by Shenzhen Science and Technology Project JCYJ20160229172341417. *(Corresponding author: Chenguang Yang.)*

C. Yang and Y. Jiang are with the Key Laboratory of Autonomous Systems and Networked Control, South China University of Technology, Guangzhou 510641, China (e-mail: cyang@ieee.org; ym.jiang2015@gmail.com).

Z. Li is with Department of Automation, University of Science and Technology of China, Hefei 230026, China (e-mail: zjli@ieee.org).

W. He is with the School of Automation and Electrical Engineering, University of Science and Technology Beijing, Beijing 100083, China (e-mail: weihe@ieee.org).

J. Na is with the Faculty of Mechanical and Electrical Engineering, Kunming University of Science and Technology, Kunming 650093, China (e-mail: najing25@163.com).

B. Xu is with the School of Automation, Northwestern Polytechnical University, Xi'an 710072, China, and also with the Research Institute of Northwestern Polytechnical University in Shenzhen, Shenzhen 518057, China (e-mail: smileface.binxu@gmail.com).

Color versions of one or more of the figures in this paper are available online at http://ieeexplore.ieee.org.

Digital Object Identifier 10.1109/TIE.2018.2803773

***Index Terms*—Adaptive control, finite time, robotic manipulator, parameter estimation, unknown kinematics and dynamics.**

I. Introduction

AS ONE of the most promising techniques, robotics have been extensively studied by industrial and academic communities in recent years [1]–[5], while automated robots have been widely allocated in the modern manufacturing and factories, e.g., YuMi made by ABB, Baxter made by Rethink, and Rolins' Justin developed by German Aerospace Agency [6]. To guarantee the control performance of the robot manipulators, whose dynamics are highly nonlinear, time varying, and strong coupling, model-based control methods were proposed by using complete robot dynamic information. Many well-performed robot controllers such as computed torque control [7], augmented proportional-derivative control [8], and impedance control [9] are model-based control and have been successfully implemented in a wide range of robot applications.

A prerequisite of the model-based control is that the robot dynamic model should be perfectly known, since an inaccurate model may lead to degradation of the control performance or even incur instability [3]. Approximation-based control approaches such as fuzzy logic control and neural network have been used to learn the robot dynamic model [10]–[12]. In these approximation-based controls, however, only uniformly ultimate boundedness of the tracking errors was proved and the convergence of the estimated weights was not guaranteed to their real values. This may lead to slow convergence speed and longer weights training process, which block the approximation-based control for practical applications. Alternatively, the Newton–Euler (NE) modeling method, which builds the robot dynamic model by using forward and backward iterations, is appreciated by modeling accuracy and computational efficiency and has been widely implemented in robot dynamic modeling [13]. In this paper, a modified NE method is used to establish the robot dynamic model.

In the NE modeling procedure, the knowledge of robot dynamic parameters is important for establishing an accurate model. However, such parameters are hardly known beforehand due to the complex robotic mechanism and uncertainties in the environment. Therefore, many techniques have been proposed to obtain the robot dynamic parameters. An early study of the

robotic dynamics identification was reported in [14], where least square (LS) methods were used to identify the unknown inertial parameters. An application of the above-mentioned work was shown in [15], where the dynamic parameters of the upper limb of a humanoid robot were successfully identified by using a modified LS identifier. An identification algorithm was proposed for flexible joint robot manipulators in [16], where accurate prediction of the joint torque has been achieved. Moreover, the estimation with uncertainties such output measurements delay and dirty derivative velocity were successfully addressed in [17]–[19]. While numerous approaches have been reported to identify the unknown dynamic parameters, few have considered the convergence rate of the estimation. Without the accurate and fast convergence of the estimated parameter, the disturbances caused by unknown robot dynamics cannot be suppressed timely, which may lead to the degeneration of the control performance and transient responses.

On the other hand, kinematic uncertainties widely exist in robot control and the nominal kinematic values may not provide accurate information in the realistic operation scenarios. In resent literature, the robot tracking control with uncertain kinematics has been reported [20], [21]. To control a robot with uncertain kinematics and gravitational force, an adaptive setpoint control scheme was proposed in [21], where the knowledge of robot Jacobian matrix was not used. A neural network robot control scheme combining with an adaptive Jacobin approximation control was presented to deal with the absence of kinematics and dynamics [22]. Although the above-mentioned adaptive schemes guaranteed the performance of the tracking control, only boundedness of the estimated parameters was obtained, whereas the convergence of the estimated parameters to their true values cannot be retained. It will be more desirable to achieve fast and accurate estimation of robot kinematic parameters rather than boundedness since we can obtain better control performance (especially transient performance) from the convergence of the estimated parameters [23].

In this paper, we develop an adaptive scheme to estimate the unknown kinematic and dynamic parameters, such that the kinematic parameters converged to their real values within a finite time, whereas the estimated errors of the dynamic parameters converged to a small neighborhood around zero in the finite time. It has been reported that the estimation performance will be improved if the adaptive laws contain the information of the estimated errors [24]. In [25], an optimal control strategy with finite-time adaptation was applied in a nonlinear system by using the dynamic programming algorithm. An adaptive estimation technique was proposed for a robot manipulator [26], where the information of estimation errors was used. Motivated by the above-mentioned works, in this paper, a set of auxiliary-filtered matrices are designed for both robot kinematic and dynamic estimation by integrating the information of the estimation errors. Comparing with the Lagrange model used in [26], the NE model used in this paper is much simpler and is more computationally efficient.

Another contribution to be highlighted is the improved accuracy of the estimated parameters by using the model reduction (MR) method. In the adaptive estimation, the persistent excitation (PE) condition is important to guarantee the convergence of the estimated parameters. However, the PE condition may not be able to satisfy when we identify the NE model of a high degree of freedom (DOF) robot (such as 7-DOF Baxter). Taking the robot dynamics $\tau = S\Phi$ for example, where S is an NE regressor matrix, Φ is a vector of dynamic parameters, and τ is the joint torque. It has been reported in [27] that some columns in the matrix S may be linearly dependent on each other due to the restriction of robotic mechanism and lack of sensors. In this regard, the regressor matrix may have a rank deficiency and consequently lead to the dissatisfaction of the PE condition. To address this problem, this paper develops an MR algorithm using two steps of singular value decompositions (SVD), such that the PE condition could be fulfilled in a relaxed manner.

It is worth to mention that the PE condition requires continuous excitation input of the robot joints, which may cause excessive actuator torque in practice. In comparison to the PE condition, the interval excitation (IE) condition only needs the interval exciting input, which greatly alleviates the requirement of the input. In this paper, the IE condition is introduced in the estimation of kinematic parameters, such that the finite-time identification is more feasible for implementation.

Main contributions of this paper are summarized as follows.

1) The construction of a novel finite-time robot control/identification scheme based on an NE model, with a leakage term driven by parameter estimation errors.
2) The designed robot controller efficiently works in the presence of dynamics uncertainties to guarantee the finite-time convergence of both tracking error and estimation error simultaneously.
3) The potential singularity problem of the NE regressor is remedied by introducing an SVD-based MR algorithm.

II. Robot Kinematics and Dynamics Modeling

In this section, we present a brief review of the robot kinematic modeling and dynamic modeling. The robot kinematics will be modeled using Denavit-Hartenberg (DH) notation, and the robot dynamic model will be built using the NE formulations.

A. Kinematic Modeling of the Robotic Manipulator

Let us define a vector of the robotic end-effector positions $x \in \mathbb{R}^{N_0}$ and a vector of joint angles $q \in \mathbb{R}^N$, where N_0 is the DOF of the task space and N is the DOF of joint space. Forward kinematics of the manipulator can be described in the following form:

$$x = f_{\text{kine}}(q). \tag{1}$$

Then, the relationship between the joint velocity $\dot{q}$ and end-effector velocity $\dot{x}$ can be obtained by taking the partial differentiation of f_{kine} as follows:

$$\dot{x} = \frac{\partial f_{\text{kine}}(q)}{\partial q}\dot{q} = J(q,\theta)\dot{q} \tag{2}$$

TABLE I
KINEMATIC AND INERTIA PARAMETERS IN NE MODELING

$m_i \in \mathbb{R}$	Mass of link i
$\tau_i \in \mathbb{R}$	The actuator torque at joint i
$\psi_i \in \mathbb{R}^3$	Angular velocity of the ith coordinate frame.
$\dot{\psi}_i \in \mathbb{R}^3$	Angular acceleration of the ith coordinate frame.
$v_i \in \mathbb{R}^3$	Line velocity of link i
$\dot{v}_i \in \mathbb{R}^3$	Line acceleration of link i
$f_{ci} \in \mathbb{R}^3$	The force at joint i caused by the motion of link i
$n_{ci} \in \mathbb{R}^3$	The torque at joint i caused by the motion of link i
$I_i \in \mathbb{R}^3$	Inertial parameters of link i

where $\theta \in \mathbb{R}^h$ are constants denoting the kinematic parameters, h denotes the number kinematics parameters, and $J(q,\theta) \in \mathbb{R}^{N_o \times N}$ is the robotic Jacobian matrix.

To facilitate the parameters estimation, the following property and assumption are considered.

Property 1 (See [22]). The Jacobian matrix $J(q,\theta)$ can be linearly parameterized as follows:

$$J(q,\theta)\dot{q} = R(q,\dot{q})\theta \tag{3}$$

where $R(q,\dot{q}) \in \mathbb{R}^{N\times h}$ is the regressor of Jacobian.

Assumption 1: The Jacobian matrix of the robotic arm is of full rank and the robot is well controlled to avoid the singularity during the estimation.

B. Dynamic Modeling of the Robotic Manipulator

The robot dynamic model is built by using the NE method. The modeling procedure consists of two recursions: a forward recursion and a backward recursion, which are derived as follows [14]. Some symbols used in the modeling procedure are given in Table I

$$\begin{aligned}
\psi_i &= {}^{i-1}_{i}R\psi_{i-1} + z_i\dot{q}_i \\
\dot{\psi}_i &= {}^{i-1}_{i}R\dot{\psi}_{i-1} + {}^{i-1}_{i}R\psi_{i-1}\times z_i\dot{q}_i + z_i\ddot{q}_i \\
\dot{v}_i &= {}^{i-1}_{i}R[\dot{v}_{i-1} + \dot{\psi}_{i-1}\times {}^{i-1}_{i}P + \psi_{i-1}\times(\psi_{i-1}\times {}^{i-1}_{i}P)] \\
f_{ci} &= m_i\dot{\varsigma}_i + \dot{\psi}_i \times m_{h_i} + \psi_i \times (\psi_i \times m_{h_i}) \\
n_{ci} &= I_i\dot{\psi}_i + \psi_i \times (I_i\psi_i) - \dot{\varsigma}_i \times m_{h_i}
\end{aligned} \tag{4}$$

where z_i is a vector of joint rotation axis, i.e., $z_i = [0,0,1]^T$, $\dot{\varsigma}_i = \dot{v}_i + \dot{\psi}_i \times v_i$, ${}^{i-1}_{i}R$ is the rotation transform matrix, and ${}^{i-1}_{i}P \in \mathbb{R}^3$ is the transformation vector. Then, the linear parameterization of (4) with respect to m_i, m_{hi}, and I_i can be given as

$$\begin{aligned}
\zeta_{ii} &= [n_{ci}^T, f_{ci}^T]^T \\
&= \begin{bmatrix} \mathbf{0} & -L(\dot{\varsigma}_i) & E(\dot{\psi}_i)+L(\psi_i)E(\psi_i) \\ \dot{\varsigma}_i & L(\dot{\psi}_i)+L(\psi_i)L(\psi_i) & \mathbf{0} \end{bmatrix} \begin{bmatrix} m_i \\ m_{h_i} \\ \mathfrak{L}(\bar{I}_i) \end{bmatrix} \\
&= A_i\Phi_i
\end{aligned} \tag{5}$$

where A_i is a matrix with a proper dimension, $\Phi_i = [m_i, m_{h_i}, \mathfrak{L}(\bar{I}_i)]^T$ is a vector of unknown inertia parameters,

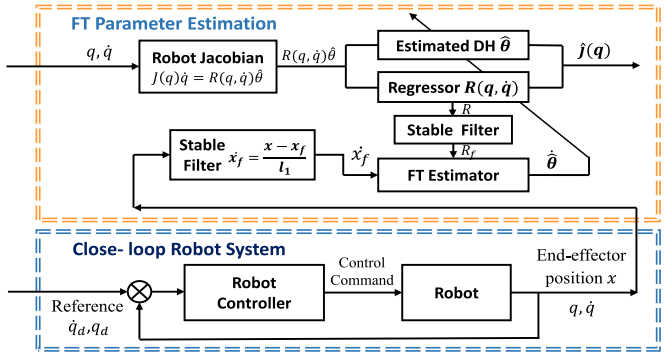

Fig. 1. Finite-time kinematics estimation strategy.

and $\mathfrak{L}(\bar{I}_i) = [I_{xx}, I_{xy}, I_{xz}, I_{yy}, I_{yz}, I_{zz}]^T$ is a vector of link inertias. $L(\cdot)$ and $E(\cdot)$ are defined as

$$L(\psi) = \begin{bmatrix} 0 & -\psi_z & \psi_y \\ \psi_z & 0 & -\psi_x \\ -\psi_y & \psi_x & 0 \end{bmatrix},$$

$$E(\psi) = \begin{bmatrix} \psi_x & \psi_y & \psi_z & 0 & 0 & 0 \\ 0 & \psi_x & 0 & \psi_y & \psi_z & 0 \\ 0 & 0 & \psi_x & 0 & \psi_y & \psi_z \end{bmatrix}.$$

It should be noted that ζ_{ii} is a force/torque at joint i exclusively depending on the movement of link i. Then, the network force ζ_i can be obtained by summarizing the torque of each link in the following manner [14], i.e., $\zeta_i = \sum_{j=i}^{N}\zeta_{ij}$, with

$$\zeta_{ij} = T_{ci}T_{ci+1}\cdots T_{cj}\zeta_{jj}, T_{ci} = \begin{bmatrix} {}^{i}_{i+1}P^{i}_{i+1}R & {}^{i}_{i+1}R \\ {}^{i}_{i+1}R & 0 \end{bmatrix}.$$

Since $\tau_i = \begin{bmatrix} z_i^T & \mathbf{0} \end{bmatrix}^T \zeta_i$ and considering (5), we can obtain the linear-in-parameterized NE formulation as follows

$$\tau = S\Phi = \begin{bmatrix} S_{11} & S_{12} & \cdots & S_{1N} \\ \mathbf{0} & S_{22} & \cdots & S_{2N} \\ \vdots & \vdots & \ddots & \vdots \\ \mathbf{0} & \mathbf{0} & \cdots & S_{NN} \end{bmatrix} \begin{bmatrix} \Phi_1 \\ \Phi_2 \\ \vdots \\ \Phi_N \end{bmatrix} \tag{6}$$

where $H_{ij} = T_{ci}T_{ci+1}\cdots T_{cj}A_i$, and particularly, $H_{ii} = A_i$. $S_{ij} = \begin{bmatrix} z_i & \mathbf{0} \end{bmatrix}^T H_{ij}$.

III. FINITE PARAMETER IDENTIFICATION SCHEME DESIGN

In this section, finite-time identification schemes are developed to obtain the robot kinematic and dynamic parameters, which are assumed to be unknown in this paper.

A. Identification of the Kinematic Parameters

Fig. 1 illustrates the kinematic estimation strategy. The unknown kinematic parameters θ would be estimated using a finite-time estimator with ensured finite-time convergence. Combining (1)–(3), we have

$$\dot{x} = J(q,\theta)\dot{q} = R(q,\dot{q})\theta. \tag{7}$$

Note that the end-effector velocity $\dot{x}$ is measured by using an external sensor, which may be sensitive to noises. To avoid using the velocity term, a stable linear filter $(\cdot)_f = \frac{1}{l_1 s+1}(\cdot)$ is adopted on both sides of (7) as follows

$$R_f(q,\dot{q})\theta = \dot{x}_f \tag{8}$$

where $R_f(q,\dot{q}) \in \mathbb{R}^{N\times h}$ is the filtered regressor matrix, and $\dot{x}_f$ is the filtered velocity satisfying the following equality,

$$\begin{cases} l_1\dot{R}_f(q,\dot{q}) + R_f(q,\dot{q}) = R(q,\dot{q}) & R_f|_{t=0} = 0 \\ l_1\dot{x}_f + x_f = x & x_f|_{t=0} = 0 \end{cases} \tag{9}$$

with l_1 being a positive constant. Then, $\dot{x}_f$ could be replaced by $\frac{(x-x_f)}{l_1}$ in terms of (9). Therefore, only position information need to be used during the estimation. Two definitions are introduced as follows.

Definition 1 (See [26]): A vector or matrix function R_f is persistently exciting (or satisfy the PE condition) if there exist $T>0, \varepsilon>0$ such that $\int_t^{t+T} R_f(r)^T R_f(r)dr \geq \varepsilon I, \forall t \geq 0$.

Definition 2 (See [28]): A bounded vector or matrix function R_f is interval exciting (or satisfy the IE condition) over an interval $[T_e - T_0, T_e]$ if there exist T_e, T_0, and ε such that $\int_{T_e-T_0}^{T_e} R_f(\tau)^T R_f(\tau)d\tau \geq \varepsilon I$ holds.

Remark 1: The PE condition is necessary to ensure the convergence of the estimated parameters. However, this condition is not easy to guarantee. In comparison to the PE condition, the IE condition only needs to hold in an interval time, which greatly alleviates the requirement.

In the following, let us introduce an auxiliary matrix $\mathcal{D} \in \mathbb{R}^{h\times h}$ and two auxiliary vectors $\mathcal{T} \in \mathbb{R}^N$ and $\mathcal{P} \in \mathbb{R}^N$ as follows:

$$\begin{cases} \dot{\mathcal{D}} &= -\vartheta\mathcal{D} + R_f(q,\dot{q})^T R_f(q,\dot{q}) \quad \mathcal{D}(0) = 0 \\ \dot{\mathcal{T}} &= -\vartheta\mathcal{T} + R_f(q,\dot{q})^T \frac{(x-x_f)}{l_1} \quad \mathcal{T}(0) = 0 \\ \mathcal{P} &= \mathcal{T} - \mathcal{D}\hat{\theta} \end{cases} \tag{10}$$

where ϑ is a positive constant representing a forgetting factor for the filter matrix, and it is designed to keep the balance between the robustness and the convergence rate.

Integrating on both sides of (10) with respect to time, the solution of $\mathcal{D}$ and $\mathcal{T}$ can be derived as follows:

$$\begin{cases} \mathcal{D}(t) &= \int_0^t e^{-\vartheta(t-r)} R_f(q(r),\dot{q}(r))^T R_f(q(r),\dot{q}(r))dr \\ \mathcal{T}(t) &= \int_0^t e^{-\vartheta(t-r)} R_f(q(r),\dot{q}(r))^T \frac{(x-x_f)}{l_1} dr. \end{cases} \tag{11}$$

Remark 2: From the definition of PE condition, we can obtain that $\int_t^{t+T} R_f^T(r)R_f(r)dr \geq \varepsilon I$, which also equals to $\int_{t-T}^{t} R_f^T(r)R_f(r)dr \geq \varepsilon I$, for $t > T > 0$. Thus, if R_f satisfies the PE condition, the relationship $\int_{t-T}^{t} R_f^T(r)R_f(r)dr \geq \varepsilon I$ will hold for $t > T > 0$. Then, let us consider the integration interval $r \in [t-T, t]$. Since $t - r \leq T$, we can obtain that $e^{-\vartheta(t-r)} \geq e^{-\vartheta T} > 0$ according to the monotonicity of the exponential function. Then, we can derive that $\int_{t-T}^{t} e^{-\vartheta(t-\tau)} R_f^T(r)R_f(r)dr \geq \int_{t-T}^{t} e^{-\vartheta T} R_f^T(\tau)R_f(\tau)dr \geq e^{-\vartheta T}\varepsilon I$. In addition, $\int_0^t e^{-\vartheta(t-r)} R_f^T(r)R_f(r)dr > \int_{t-T}^{t} e^{-\vartheta(t-r)} R_f^T(r)R_f(r)dr$ holds for all $t > T > 0$. From the above-mentioned analysis, we have $\mathcal{D} = \int_0^t e^{-\vartheta(t-r)} R_f^T(r)R_f(r)dr > e^{-\vartheta T}\int_{t-T}^{t} R_f^T(r)R_f(r)dr \geq e^{-\vartheta T}\varepsilon I$. This implies that $\mathcal{D}$ is positive definite and its minimum eigenvalue satisfies $\lambda_{\min}(\mathcal{D}) > \sigma$ with $\sigma = e^{-\vartheta T}\varepsilon$.

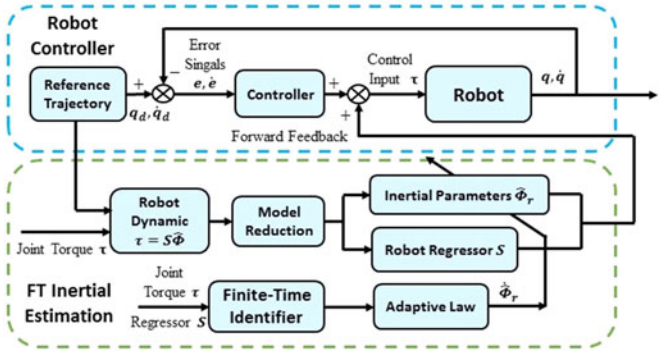

Fig. 2. Finite-time dynamic estimation strategy of a robot manipulator.

Remark 3: Comparing the structure between $\mathcal{D}(t)$ and $\mathcal{T}(t)$ in (11), and in terms of (8), we can obtain that $\mathcal{T} = \mathcal{D}\theta$. Hence, $\mathcal{P}$ can be represented by $\mathcal{P} = \mathcal{D}\theta - \mathcal{D}\hat{\theta} = \mathcal{D}\tilde{\theta}$. This implies that $\mathcal{P}$ contains the information of the estimated error $\tilde{\theta}$.

Then, the updating law for $\hat{\theta}$ is designed as follows:

$$\dot{\hat{\theta}} = \begin{cases} -\Gamma\dfrac{\mathcal{P}}{||\mathcal{P}||} & \text{if } P \neq 0 \\ 0 & \text{if } P = 0 \end{cases} \tag{12}$$

where Γ is a positive constant to be specified by the designer. Note that in the estimation of kinematic parameters, the end-effector position x and the joint variables q, $\dot{q}$ are assumed to be bounded and available. This can be achieved via an internal position controller of the robot manipulator.

Theorem 1: Consider the robotic kinematics model (3), assume that $R_f(q,\dot{q})$ satisfies the IE condition $\int_{T_e-T_0}^{T_e} R_f(\tau)^T R_f(\tau)(\tau)d\tau \geq \varepsilon I$ for some positive constants T_e, T_0, and ε. Then, the estimation error of kinematic parameters will converge to the origin in a finite time t_a under the parameter estimation law (12), satisfying $t_a \leq ||\tilde{\theta}(0)||\lambda_{\max}(\Gamma^{-1})/\sigma + T_e$, with σ being a positive value, $\lambda_{\max}(\bullet)$ being the maximum matrix eigenvalue.

Proof. Please see Appendix A. ■

B. Identification of the Dynamic Parameters

In this part, an adaptive estimation scheme will be developed to identify the unknown dynamic parameters. The estimation strategy is demonstrated in Fig. 2.

1) Auxiliary Matrix Design: Similar to the identification process in Section III-A, a group of auxiliary matrix is constructed for the dynamic identification as follows:

$$\begin{cases} \dot{U} = -\delta U + S^T S & U(0) = 0 \\ \dot{B} = -\delta B + S^T \tau & B(0) = 0 \\ E = B - U\hat{\Phi} \end{cases} \tag{13}$$

where δ is a positive constant to be specified. The solution of U and B can be derived as $U(t) = \int_0^t e^{-\delta(t-r)} S^T(r)S(r)dr, B(t) = \int_0^t e^{-\delta(t-r)} S^T(r)\tau dr$.

Note that in the estimation, the PE condition may not be satisfied since $U(t)$ may not be full rank [15]. To solve this problem, an SVD-MR method is developed as follows.

2) SVD-MR: As for a common robotic arm, the unknown inertial parameters can be categorized into three groups, i.e., parameters absolutely identifiable, parameters unidentifiable, and parameters identified in linear combinations [29]. The main idea is to build a minimum set of inertial parameters through the following three steps.

1) Eliminating the zero elements columns of U.
2) Recombining the linear identifiable columns in U and then eliminating the columns that have no effect on the joint torque.
3) Rearranging and selecting the inertial parameters Φ.

Assuming that the rank of matrix U is $\text{rank}(U) = \zeta_r$, applying the SVD on the matrix U, we have

$$U = VAY^T = V \begin{bmatrix} \Sigma & \mathbf{0} \\ \mathbf{0} & \mathbf{0} \end{bmatrix} \begin{bmatrix} Y_1^T \\ Y_2^T \end{bmatrix} \tag{14}$$

where $V \in \mathbb{R}^{\zeta_u \times \zeta_u}$ and $Y = [Y_1^T, Y_2^T]^T \in \mathbb{R}^{\zeta_u \times \zeta_u}$ are orthogonal matrices, $\Sigma \in \mathbb{R}^{\zeta_r \times \zeta_r}$ is a matrix of principal elements, ζ_u is a constant denoting the dimension of U. $Y_1 \in \mathbb{R}^{\zeta_u \times \zeta_r}$ and $Y_2 \in \mathbb{R}^{\zeta_u \times (\zeta_u - \zeta_r)}$ are the submatrices.

From (14) we have $B(t) = U(t)\Phi = V\Sigma Y_1^T \Phi = \int_0^t e^{-\delta(t-r)} S^T(r)\tau dr$. Thus, we can derive that the matrix Y_2 and zero rows in Y_1 would not affect the output of $B(t)$. Hence, the corresponding inertial parameters can be grouped into the unidentifiable parameters. On the other hand, since $[Y_1^T, Y_2^T]^T$ is an orthogonal matrix, thus the subspace of zero columns in Y_2^T corresponds to the subspace of linearly independent columns in Y_1^T, which means that we can find the absolutely identifiable inertial parameters Φ through the zero columns in Y_2^T. Then, the rest of inertial parameters can be grouped into linear identifiable parameters.

After the categorization of the three groups' inertial parameters, we need to obtain the combinations form of the linear identifiable parameters Φ_c. Then, an augment matrix U_r is designed by eliminating the columns of U, which are corresponding to the unidentifiable parameters and absolutely identifiable parameters. Assume that the rank of U_r is $\text{rank}(U_r) = \zeta_{r_2}$, then an SVD is further employed on U_r as follows:

$$U_r = V_r A_r Y_r^T = V_r \begin{bmatrix} \Sigma_r & \mathbf{0} \\ \mathbf{0} & \mathbf{0} \end{bmatrix} \begin{bmatrix} Y_{r1}^T \\ Y_{r2}^T \end{bmatrix} \tag{15}$$

where $\Sigma_r \in \mathbb{R}^{\zeta_{r_2} \times \zeta_{r_2}}$ is a diagonal matrix. $Y_{r1} \in \mathbb{R}^{\zeta_{u2} \times \zeta_{r2}}$ and $Y_{r2} \in \mathbb{R}^{\zeta_{u2} \times (\zeta_{u2} - \zeta_{r2})}$ are the submatrices and ζ_{u2} is a constant denoting the dimension of U_r. The rows of matrix Y_{r2} (and the corresponding elements in Φ_c) can be rearranged as follows [27]:

$$P^T Y_{r2}^T = \begin{bmatrix} Y_{r21}^T \\ Y_{r22}^T \end{bmatrix} \quad P^T \Phi_c = \begin{bmatrix} \Phi_1 \\ \Phi_2 \end{bmatrix} \tag{16}$$

where P is a selecting permutation matrix to guarantee Y_{r22}^T to be a regular matrix, $\Phi_1 \in \mathbb{R}^{\zeta_{u2} - \zeta_{r2}}$ and $\Phi_2 \in \mathbb{R}^{\zeta_{r2}}$ are the subvectors. Premultiplying P^T on Φ_c as shown in the right-hand side of (16), we can derive the detailed form of the linear identifiable parameters $\Phi_c^{'}$ as $\Phi_c^{'} = \Phi_1 - \beta\Phi_2$, where $\beta = Y_{r21}Y_{r22}^{-1}$ is the coefficient matrix of the linear combinations. Then, the argument parameters set Φ_r could be obtained by adding Φ_a to $\Phi_c^{'}$ as $\Phi_r = [\Phi_a, \Phi_c^{'}]^T$. The corresponding regressor matrix S_r can be obtained by choosing the corresponding columns in S. Thus, the NE equation (6) could be reconstructed as $\tau = S_r\Phi_r$.

Remark 4: It should be emphasized that the regrouping of inertial parameters would not change the calculation result of the joint torque, i.e., $\tau = S_r\Phi_r = S\Phi$, since the deleted parameters and the corresponding columns in S have no contribution to the joint torque [27].

3) Finite-Time Estimation Design: Subsequently, we will introduce an alternative FT adaptive law to estimate the parameters Φ_r. Let us define an auxiliary matrix Q, where the time derivative of Q is given as follows:

$$\dot{Q} = \delta Q - QS_r^T S_r Q, \quad Q(0) = Q_0^{-1} > 0 \tag{17}$$

and $\delta > 0$ is a positive constant. Note that the following matrix equality exists: $\frac{d}{dt}QQ^{-1} = \dot{Q}Q^{-1} + Q\dot{Q}^{-1} = 0$. Multiplying Q^{-1} on both side of (17) and considering the above-mentioned equality, we have

$$\begin{aligned} Q^{-1}\dot{Q}Q^{-1} &= -Q^{-1}Q\dot{Q}^{-1} = \delta Q^{-1}QQ^{-1} \\ &\quad - Q^{-1}QS_r^T S_r QQ^{-1} = \delta Q^{-1} - S_r^T S_r. \end{aligned} \tag{18}$$

Then, the solution of the first-order differential equation (18) can be obtained as $Q^{-1}(t) = e^{-\delta t}Q_0 + \int_0^t e^{-\delta(t-r)} S_r^T(r)S_r(r)dr$, where the initial condition $Q_0 = Q^{-1}(0) > 0$ is used, selected as $Q_0 = \eta I$, η is a positive constant. Since $\mathcal{U}_c = \int_0^t e^{-\delta(t-r)} S_r^T(r)S_r(r)dr$, we have $Q(t) = \left[e^{-\delta t}Q_0 + \mathcal{U}_c(t)\right]^{-1}$.

Then, let us employ the SVD for the matrix $\mathcal{U}_c$ as $\mathcal{U}_c = \mathcal{V}_c\mathcal{A}_c\mathcal{Y}_c^T$, where $\mathcal{V}_c$ is an orthogonal matrix whose columns are eigenvectors of $\mathcal{U}_c\mathcal{U}_c^T$, $\mathcal{Y}_c$ is an orthogonal matrix whose columns are eigenvectors of $\mathcal{U}_c^T\mathcal{U}_c$, and $\mathcal{A}_c$ is a diagonal matrix of the form $\mathcal{A}_c = \text{diag}\{a_1, \ldots, a_n\}$. Note that the matrix $\mathcal{V}_c$ and $\mathcal{Y}_c$ are unitary matrices such that the relationships $\mathcal{V}_c\mathcal{V}_c^T = I$ and $\mathcal{Y}_c\mathcal{Y}_c^T = I$ hold. Then, it follows that

$$\begin{aligned} Q &= \left[e^{-\delta t}Q_0 + \mathcal{U}_c\right]^{-1} = \left[\mathcal{V}_c(\mathcal{A}_c + e^{-\delta t}\eta I)\mathcal{Y}_c^T\right]^{-1} \\ &= \mathcal{Y}_c(\mathcal{A}_c + e^{-\delta t}\eta I)^{-1}\mathcal{V}_c^T. \end{aligned} \tag{19}$$

Since $\mathcal{V}_c$ satisfies that $\mathcal{V}_c^{-1} = \mathcal{V}_c^T$, we can obtain that $\mathcal{V}_c^T\mathcal{U}_c = \mathcal{A}_c\mathcal{Y}_c^T$. Then, multiplying $\mathcal{U}_c$ on both side of (19), we have

$$\begin{aligned} Q\mathcal{U}_c &= \mathcal{Y}_c(\mathcal{A}_c + e^{-\delta t}\eta I)^{-1}\mathcal{V}_c^T\mathcal{U}_c \\ &= \mathcal{Y}_c(\mathcal{A}_c + e^{-\delta t}\eta I)^{-1}\mathcal{A}_c\mathcal{Y}_c^T \\ &= \mathcal{Y}_c \,\text{diag}\left(\frac{a_1}{a_1 + e^{-\delta t}\eta}, \ldots, \frac{a_n}{a_n + e^{-\delta t}\eta}\right)\mathcal{Y}_c^T. \end{aligned} \tag{20}$$

It should be noted that $\mathcal{A}_c$ is a diagonal matrix in the above-mentioned equation.

Let us define an auxiliary term $F(t)$ as follows:

$$F(t) = \mathcal{Y}_c \operatorname{diag}\left(\frac{e^{-\delta t}\eta}{a_1 + e^{-\delta t}\eta}, \ldots, \frac{e^{-\delta t}\eta}{a_n + e^{-\delta t}\eta}\right)\mathcal{Y}_c^T. \quad (21)$$

Then, (20) can be rewritten as follows:

$$Q(t)\mathcal{U}_c(t) = I - F(t). \quad (22)$$

Note that for the nonzero eigenvalue a_i, the term $\frac{e^{-\delta t}\eta}{a_i + e^{-\delta t}\eta}$ would converge to zero when $t \to \infty$. Then, we have

$$\tilde{\Phi}_r = \Phi_r - \hat{\Phi}_r = [Q\mathcal{U}_c + F]\,\Phi_r - \hat{\Phi}_r. \quad (23)$$

Now the estimated errors could be expressed by (23), which will be used to design the adaptive law in the next section.

IV. Adaptive Finite-Time Robot Control Design

Based on the NE dynamic model and the finite-time identification, in this section, we aim to control the robot to track a desired trajectory in the presence of dynamics uncertainties. The dynamics of a robot manipulator can be described as follows:

$$M(q)\ddot{q} + C(q,\dot{q})\dot{q} + G(q) = S_r(\ddot{q},\dot{q},q)\Phi_r = \tau \quad (24)$$

where $q \in \mathbb{R}^N$ is the vector of joint position, $M(q) \in \mathbb{R}^{N\times N}$ is a symmetric inertia matrix, $C(q,\dot{q})\dot{q} \in \mathbb{R}^N$ denotes the centripetal and Coriolis matrix, $G(q) \in \mathbb{R}^{N\times N}$ is a gravity force, and $\tau \in \mathbb{R}^N$ is the joint torque. Before processing the control design, we introduce two residual error signals as follows:

$$e_q = q - q_d, \qquad e_s = \dot{q} - \dot{q}_r \quad (25)$$

where q_d is the reference joint position trajectory, whereas $\dot{q}_r$ is reference velocity, which is defined as $\dot{q}_r = \dot{q}_d + \lambda e_q$, and λ is a positive constant. Substituting the definition into (25), e_s could be rewritten as $e_s = \dot{e}_q + \lambda e_q$.

To facilitate formulation, the following property of the robot control and assumption are introduced.

Property 2: The matrix $M(q)$ is symmetric and positive definite while the matrix $\dot{M}(q) - 2C(q,\dot{q})$ is skew-symmetric.

Assumption 2: The reference joint position trajectory q_d and its derivatives $\dot{q}_d$ are continuous and bounded.

Substituting (25) into (24), we have

$$M(q)\dot{e}_s + C(q,\dot{q})e_s = \tau - S_r(\ddot{q}_r,\dot{q}_r,\dot{q},q)\Phi_r. \quad (26)$$

Then, let us design the control signal as follows:

$$\tau = -K_1 e_s + S_r(\ddot{q}_r,\dot{q}_r,\dot{q},q)\hat{\Phi}_r + \tau_r \quad (27)$$

where τ_r is the robust term defined as

$$\tau_r = \begin{cases} -K_2\frac{e_s}{\|e_s\|} & (e_s \neq 0) \\ 0 & (e_s = 0) \end{cases}$$

K_1 and K_2 are the selected positive control gains. Substituting controller (27) into (26), the error dynamics could be formulated as follows:

$$M(q)\dot{e}_s + C(q,\dot{q})e_s = -K_1 e_s + S_r(\ddot{q}_r,\dot{q}_r,\dot{q},q)\tilde{\Phi}_r + \tau_r. \quad (28)$$

Fig. 3. Overlook of the Baxter robot.

TABLE II
DH Convention Table of the Baxter Left Robotic Arm

Link i	θ_i (deg)	d_i (m)	a_{i-1} (m)	α_{i-1} (rad)
1	q_1	0	0	0
2	$q_2 + \pi/2$	0	a_1	$-\pi/2$
3	q_3	d_3	0	$\pi/2$
4	q_4	0	a_3	$-\pi/2$
5	q_5	d_5	0	$\pi/2$
6	q_6	0	a_5	$-\pi/2$
7	q_7	d_7	0	$\pi/2$

The adaptive law can be designed as follows:

$$\dot{\hat{\Phi}}_r = \begin{cases} -\Gamma_d\left(S_r^T e_s - \frac{\hat{\Phi}_r - QB_c}{\|\hat{\Phi}_r - QB_c\|}\right) & \text{if} \quad \|\hat{\Phi}_r - QB_c\| \neq 0 \\ -\Gamma_d S_r^T e_s & \text{if} \quad \|\hat{\Phi}_r - QB_c\| = 0 \end{cases} \quad (29)$$

where Γ_d is a positive constant, $B_c = \int_0^t e^{-\delta(t-r)} S_r^T(r)\tau dr$.

Theorem 2: Consider the robotic dynamic model (24) with the controller (27) and FT adaptation law in (29) and employ the generated excitation trajectory. It could be derived that the tracking error converges to a small neighborhood around the origin, and the estimated errors $\tilde{\Phi}_r$ converges to a small compact set around zero within a finite time.

Proof. Please see Appendix B. ■

V. Simulation and Experiment Study

To illustrate the effectiveness of the proposed algorithms, simulations and experiments are carried out based on a 7-DOF Baxter robot arm as shown in Fig. 3.

A. Kinematics FT Estimation and Verification

1) Simulation Setup: The coordinate frames of the 7-DOF Baxter robot are shown in Fig. 3. For a chain of revolute joints, the DH notation was used to build the kinematics model as listed in Table II, and the nominal values are $a_1 = 0.069$, $a_3 = 0.069$, $a_5 = 0.01$, $d_3 = 0.36435$, $d_5 = 0.37429$, and $d_7 = 0.22953$. These parameters are assumed to be unknown and will be estimated using the FT adaptation law (12). During the kinematic estimation, the Baxter robot would run in the position control module such that the velocity of each joint is stable and bounded.

The Baxter robot is commanded to track the reference trajectory $q_{di} = a_i\cos(0.3t + b_i\pi) + c_i$, where $a_1 = a_2 = 0.1$, $a_3 = a_4 = 0.3$, $a_5 = a_6 = a_7 = 0.5$, $b_1 = 0, b_2 = 0.4$, $b_3 = 0.1, b_4 = 0.3, b_5 = 0.6, b_6 = 0.8, b_7 = 0.5$, $c_1 = 0.2$,

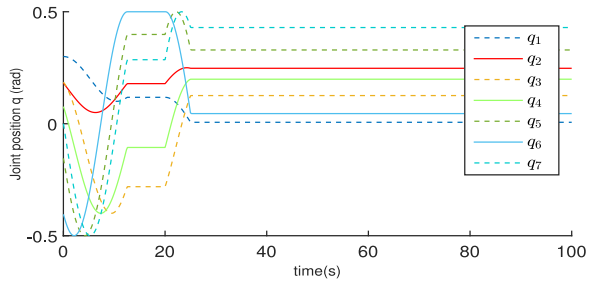

Fig. 4. Input signals with IE.

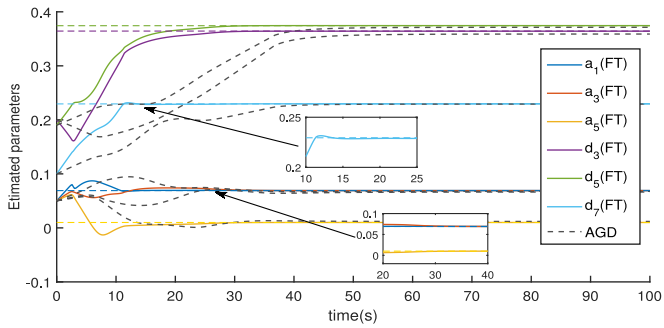

Fig. 5. Convergence of the estimate parameters in the interval time.

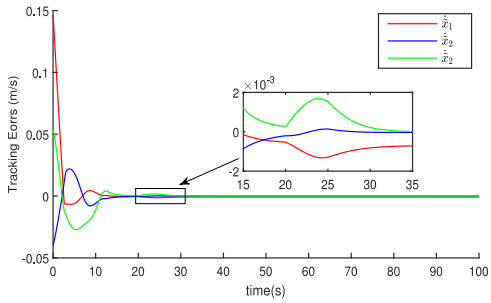

Fig. 6. Tracking performance.

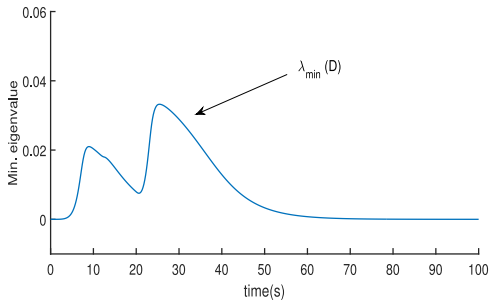

Fig. 7. Minimum eigenvalue of the auxiliary matrix $\mathcal{D}$.

$c_2 = 0.15, c_3 = c_4 = -0.1, \quad c_5 = c_6 = c_7 = 0,$ which is excited during the period 0–12 s and 18–24 s, and remains unchanged during 12–18 s. The gains are set to $\vartheta = 0.015$, $\Gamma = 0.025, l_1 = 0.01$. The initial values of the estimated parameters are selected to $\hat{\theta}(0) = [0.05, 0.05, 0.05, 0.2, 0.19, 0.1]^T$.

2) Simulation Results: Results of the kinematic estimation are shown in Figs. 4–7. Fig. 4 illustrates the joint velocities of the robot, which satisfied the IE condition. We can see that $\dot{q}_i$ is excited during the time interval 0–12 s and 18–24 s, and during the period 12–18 s the inputs stay the same. Parameters estimation performance is shown in Fig. 5, and the tracking errors are shown in Fig. 6. It can be seen from Fig. 5 that all the estimated DH parameters (solid line "−") converge to their true values (dashed line "−−") with fast convergence rate. Even the inputs are keeping silent for a short period of time, the proposed algorithm can still guarantee the estimation performance. Comparing with the adaptive gradient descent method as shown in Fig. 5, the estimation performance of the proposed FT algorithm is much better in both convergence speed and accuracy. Fig. 7 shows the profile of the minimum eigenvalue of the auxiliary matrix $\mathcal{D}$.

As shown in Fig. 7, the minimum eigenvalue of the $\mathcal{D}$ rises during the periods 1–12 s and 18–24 s, and reaches to the peak at about 24 s, which verified the satisfaction of IE condition. This also shows that the proposed algorithm could effectively work under the interval exciting inputs.

3) Robustness Verification and Experiment: To further show the effectiveness of our proposed estimation algorithm, robustness tests are conducted by adding unknown external disturbances to the system model. In some practical applications, uncertainties may inevitably exist in the measurement of end-effector position, e.g., the camera-based object tracking system may easily be affected by environmental noises. In the comparative studies, we conduct the test by adding the white noises with different intensity to the measured end-effector position. The external disturbance is chosen to be $d(t) = \sigma w(t)$, where σ is the degree of intensity, and $w(t)$ is the white Gaussian noise with the power of 1 dBW. For fair comparisons, the parameters in the adaptive estimation are chosen the same and robot is tracking the same trajectories.

The simulation results are depicted as shown in Figs. 8–13. The disturbances added on the measured end-effector position are shown in Figs. 8, 10, and 12, with σ chosen to be $\sigma = 0.005$, $\sigma = 0.01$, and $\sigma = 0.02$. It can be observed from the figures that the maximum deviations added on the measured positions are about ± 2 cm, ± 4 cm, and ± 6 cm, respectively. The parameters estimation performance are shown in Figs. 9, 11, and 13. We can see from the figures that the parameters of three groups are observed with satisfactory convergence rate and accuracy, even in the presence of external disturbances.

In addition, experiments have been further performed based on the left robotic arm of a real Baxter robot, as shown in Fig. 3. In the experiment, the robot is commanded to track a set of sinusoidal and cosine trajectories depicted in Fig. 14. The estimation results are shown in Fig. 15. We can see from the figure that most of the estimated parameters are close to the nominal values (dashed line) and observed with satisfactory convergence performance. Thus, the robustness of the proposed estimation algorithm can be verified.

B. Adaptive FT Dynamics Estimation and Control

A numerical experiment is further conducted to verify the dynamic parameters estimation. The initial NE model of Baxter

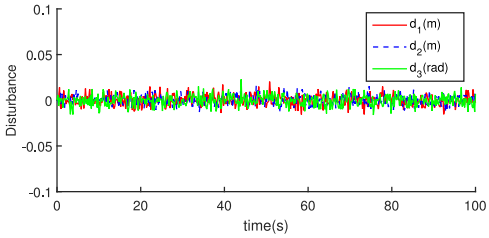

Fig. 8. Added disturbances on the end-effector position $\sigma = 0.005$.

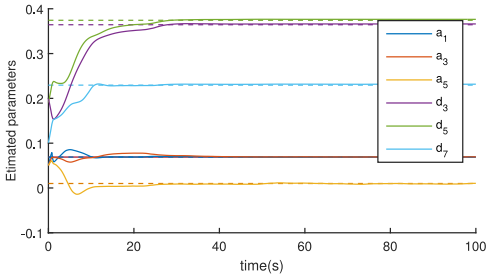

Fig. 9. Kinematics estimation performance with the disturbance $\sigma = 0.005$.

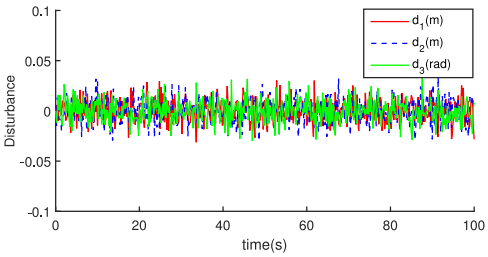

Fig. 10. Added disturbances on the end-effector position ($\sigma = 0.01$).

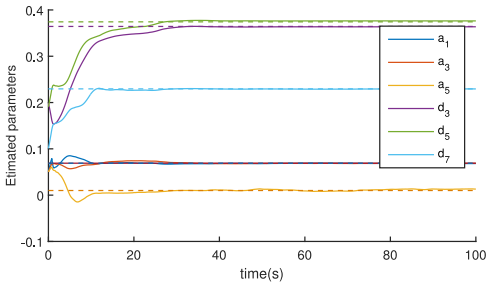

Fig. 11. Kinematics estimation performance with the disturbance ($\sigma = 0.01$).

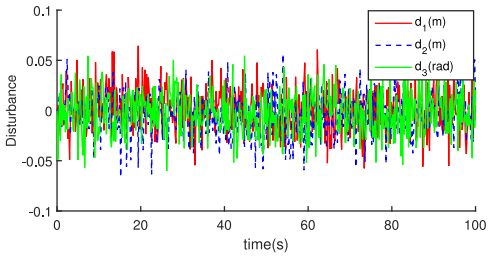

Fig. 12. Added disturbances on the end-effector position ($\sigma = 0.02$).

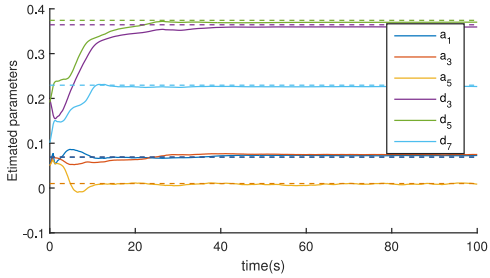

Fig. 13. Kinematics estimation performance with the disturbance ($\sigma = 0.02$).

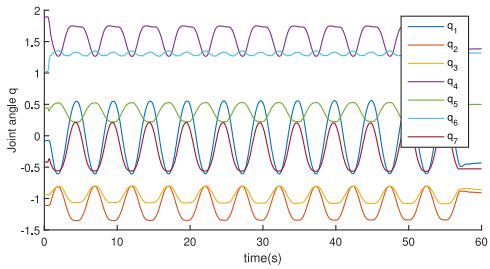

Fig. 14. Trajectories of the joint angles.

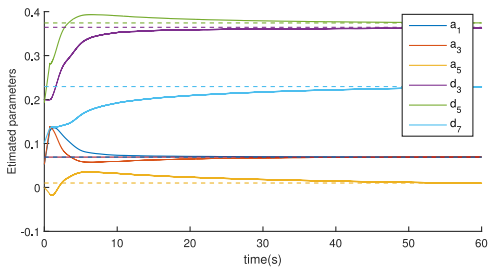

Fig. 15. Kinematics estimation performance of the experiments.

robot contains 70 inertial parameters. After MR, these parameters are recombined into 43 parameters with 22 absolutely identifiable parameters and 21 linear combinations of the linearly identifiable parameters. Periodic and bandlimited excitation joint reference trajectories $\ddot{q}_d$, $\dot{q}_d$, q_d are generated by using the Fourier expansion to guarantee the excitation condition [15].

The control gains are chosen as $k_1 = \text{diag}\,[320, 185, 40, 42, 5, 10, 0.38]$, $k_2 = \text{diag}\,[26, 19, 3, 5, 0.4, 0.75, 0.03]$. The gains of the adaptation law are selected to be $\Gamma_d = 20$ and $\delta = 2$. The initial parameters of $\hat{\Phi}_r$ are selected to be zero. The initial states of q, $\dot{q}$, and $\ddot{q}$ are set to zero.

The estimation results are depicted as shown inFigs. 16–25, where Figs. 16–22 show the robot tracking performance and Figs. 24 and 25 show the parameters estimation performance. We can see from the figures that the robot follows the reference trajectories well by using our proposed finite-time estimation algorithm, and satisfactory transient performances are observed.

To further verify the effectiveness of the proposed algorithm, comparison studies have been carried out based on a PID controller, an adaptive controller in [26], and the proposed controller, respectively. The comparative results are depicted in Figs. 16–23. As seen from the figures, although stable tracking performance can be obtained by all three types of controllers, the tracking errors of the PID control (dashed-dotted line "–.") are

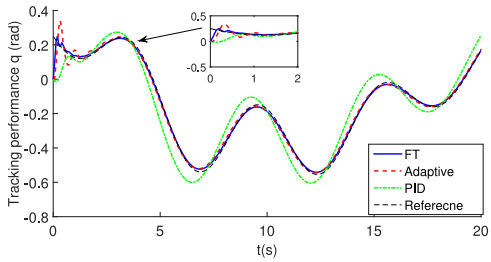

Fig. 16. Tracking performance of Joint 1.

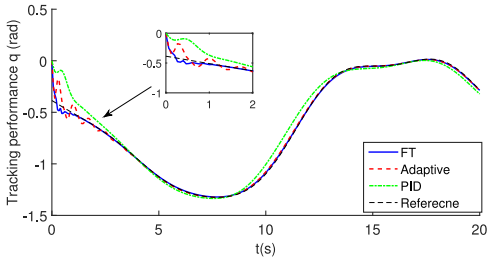

Fig. 17. Tracking performance of Joint 2.

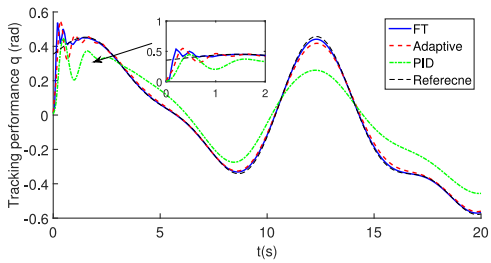

Fig. 18. Tracking performance of Joint 3.

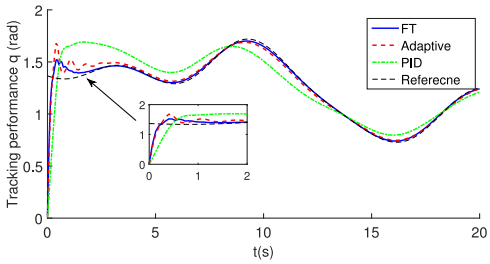

Fig. 19. Tracking performance of Joint 4.

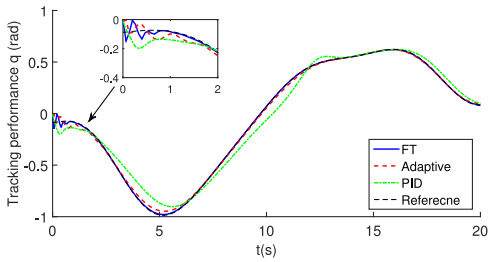

Fig. 20. Tracking performance of Joint 5.

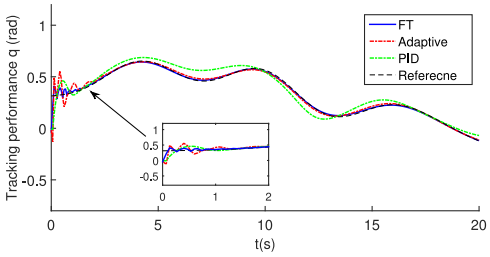

Fig. 21. Tracking performance of Joint 6.

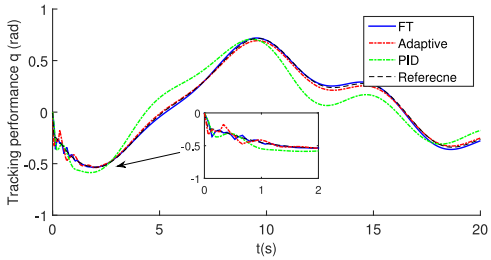

Fig. 22. Tracking performance of Joint 7.

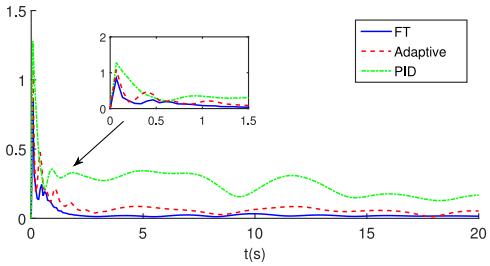

Fig. 23. RMSE of the tracking error.

relatively large, and the control performance of the FT method is superior to the PID controller in both transient and steady stages. Comparing with the adaptive controller, the tracking errors under the proposed controller converged faster than the adaptive control method and are observed with better transient control performance. This is because that the MR algorithm used in this paper can reduce the redundant information of the NE robot dynamic model and result in better estimation performance. Fig. 23 shows the profile of the root-mean-square error (RMSE) of tracking errors of the seven joints. We can see clearly from the figure that both steady-state and transient errors are improved than the other two, which verify the effectiveness of the proposed controller.

To further validate the parameter estimation performance, the RMSE of the estimated parameters is introduced as $e_{\text{RMSE}} = \sum_{i=1}^{n} \sqrt{(\hat{\Phi}_i - \Phi_i)^2/n}$, where n is the parameters number. The parameters estimation performance is depicted as shown in Figs. 24–25. As seen from Fig. 24, all the estimated inertial parameters could converge to a small bound of their true values in a short time, whereas in Fig. 25, the two subfigures show that the profiles of RMSE converge to a small neighborhood around zero. Comparisons of the parameter estimation performance have also been carried out based on our proposed FT estimated algorithm and the adaptive estimation method in [26]. The details of the estimated parameters are shown in Table III, where the real values, the parameters estimated by using our proposed finite-time algorithm, and adaptive estimation method in [26]

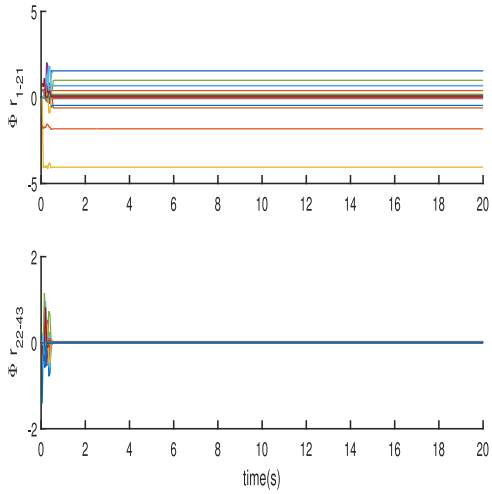

Fig. 24. Estimation performance of the inertial parameters with the proposed method.

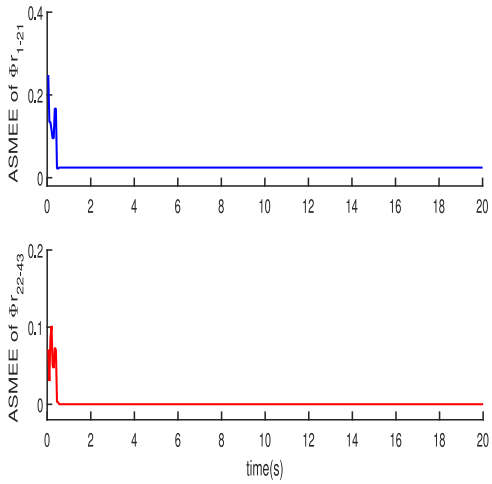

Fig. 25. RMSE of the estimated inertial parameters.

have been presented, respectively. We can see from Table III that the parameters estimated by using our proposed method is close to the real dynamic parameters, and has more estimation accuracy than conventional adaptive estimation method.

Remark 5: In this paper, we investigated the parameters estimation of the unknown robot dynamics based on the NE model. The SVD-based MR algorithm has been used to remove the redundant information in the NE model, such that the efficiency and accuracy of the parameters estimation have been improved. In comparison with the estimation method in [26], the NE model used in this paper is much simpler and more suitable for the real-time estimation of a high DOF robot.

VI. Conclusion

Based on a novel parameter identification scheme, this paper developed a robot controller in the presence of unknown kinematics and dynamics. The DH method was employed to build the kinematic model of a robot, whereas the recursive NE formulation was applied to build the robot dynamic model. Finite-time identifiers were developed to estimate the unknown kinematic and dynamic parameters with guaranteed finite-time convergence. An MR technique was introduced to relax the PE condition in the identification of robot dynamic parameters. Simulation and experimental results demonstrated that the proposed method could guarantee the convergence of the estimated parameters to a small neighborhood of their real values in the finite time, which verified the effectiveness of the proposed controller.

TABLE III
Estimation Performance of Dynamic Parameters

No.	Real	Proposed	Adaptive	No.	Real	Proposed	Adaptive
1	0.0689	0.1322	0.0864	23	0.0208	0.0205	0.0084
2	− 0.2773	− 0.6104	− 1.4653	24	0.0118	0.0110	0.0105
3	− 4.1237	− 4.0514	− 3.4160	25	0.0021	0.0032	0.0338
4	1.5528	1.5552	1.3533	26	0.0284	0.0283	0.0063
5	0.6692	0.9955	1.8549	27	− 0.0011	− 0.0015	0.0344
6	1.5244	1.5274	1.4008	28	0.0033	0.0032	− 0.0114
7	− 0.0253	0.0211	0.1150	29	0.0093	0.0091	0.0345
8	0.1696	0.1666	0.0683	30	0.0071	0.0069	0
9	0.4057	0.3986	0.4159	31	0.0007	0.0013	0.0047
10	0.0168	0.0600	0.0580	32	0.0168	0.0166	− 0.0086
11	− 0.0241	− 0.0670	− 0.1071	33	0.0006	− 0.0007	0.0146
12	0.0087	0.0334	0.0360	34	0.0112	0.0110	0.0016
13	0.0027	− 0.0051	0.0484	35	0.0054	0.0055	0.0021
14	0.0332	0.0839	0.0266	36	0.0039	0.0031	0.0226
15	− 0.4721	− 0.4638	1.4161	37	− 0.0002	− 0.0008	0.0109
16	− 1.8565	− 1.8240	− 1.1679	38	0.0028	0.0027	0.0088
17	− 0.0162	− 0.0153	− 0.0279	39	0.0005	0.0005	0.0013
18	0.7035	0.6918	0.4194	40	0.0009	0.0009	− 0.0030
19	0.1869	0.1836	− 0.2221	41	0.0005	0.0007	0.0044
20	0.6905	0.6790	0.3696	42	0.0001	0.0001	0.0179
21	− 0.0246	0.0217	0.1070	43	0.0002	0.0002	0.0117
22	0.0087	0.0085	− 0.0214				

Appendix A
Proof of Theorem 1

Let us consider a Lyapunov function as follows:

$$L_k = \frac{1}{2}\tilde{\theta}^T \Gamma^{-1} \tilde{\theta}. \tag{30}$$

Considering $\mathcal{P} = \mathcal{D}\theta - \mathcal{D}\hat{\theta} = \mathcal{D}\tilde{\theta}$, in the case of $\mathcal{P} = 0$, $T \geq T_e$, and the positiveness of $\mathcal{D}$ under IE condition, the parameter estimated error $\tilde{\theta}$ would converge to zero. In the case of $\mathcal{P} \neq 0$, let us differentiate (30) with respect to time and substituting (12) into it yields $\dot{L}_k = \tilde{\theta}^T \Gamma^{-1} \dot{\tilde{\theta}}$. Substituting the adaptive law $\dot{\hat{\theta}} = -\Gamma \frac{\mathcal{P}}{||\mathcal{P}||}$, we have $\dot{L}_k = -\tilde{\theta}^T \frac{\mathcal{P}}{||\mathcal{P}||} = -\frac{\tilde{\theta}^T \mathcal{D}\tilde{\theta}}{||\mathcal{D}\tilde{\theta}||}$. Notice that the matrix $\mathcal{D}$ is positive definite, thus all singular values of $\mathcal{D}$ are great than zero. Considering $\tilde{\theta}$ is a vector, thus we can derive property that $\tilde{\theta}^T \mathcal{D}\tilde{\theta} \geq \lambda_{\min}(D)\tilde{\theta}^T\tilde{\theta}$. Then, we have $\dot{L}_k = -\frac{\tilde{\theta}^T \mathcal{D}\tilde{\theta}}{||\mathcal{D}\tilde{\theta}||} \leq -\frac{\lambda_{\min}(D)}{\lambda_{\max}(D)}||\tilde{\theta}|| \leq -\mu\sqrt{L_k}$, with $\mu = \sqrt{\frac{\lambda_{\min}(D)}{\lambda_{\max}(D)}}/\lambda_{\max}(\Gamma^{-1})$. As the IE condition is satisfied, we can derive $\mathcal{D} > \sigma I$ in terms of (11) and the Definition 2, hence, there is always a positive constant μ such that $\mu \geq \sqrt{\frac{\lambda_{\min}(D)}{\lambda_{\max}(D)}}/\lambda_{\max}(\Gamma^{-1})$. According to the result in [30], we can obtain that $\tilde{\theta}$ could converge to zero within finite time $t_a \leq 2\sqrt{L_k(0)}/\mu + T_e$. ■

APPENDIX B
PROOF OF THEOREM 2

Let us consider the following Lyapunov candidate:

$$L_d = \frac{1}{2}e_s^T M e_s + \frac{1}{2}\tilde{\Phi}_r^T \Gamma_d^{-1}\tilde{\Phi}_r. \tag{31}$$

Taking the time deviation of L_d, we can obtain that

$$\dot{L}_d = e_s^T M\dot{e}_s + \frac{1}{2}e_s^T \dot{M}e_s + \tilde{\Phi}_r^T \Gamma_d^{-1}\dot{\tilde{\Phi}}_r. \tag{32}$$

Then, substituting (28) into (32) obtains

$$\begin{aligned}\dot{L}_d = \; & e_s^T(-K_1 e_s + S_r(\ddot{q}_r, \dot{q}_r, \dot{q}, q)\tilde{\Phi}_r + \tau_r) - e_s^T C(q,\dot{q})e_s \\ & + \frac{1}{2}e_s^T \dot{M}e_s + \tilde{\Phi}_r^T \Gamma_d^{-1}\dot{\tilde{\Phi}}_r.\end{aligned} \tag{33}$$

According to Property 2, and substituting the adaptation law (29) into (33), we have

$$\begin{aligned}\dot{L}_d &\le e_s^T(-K_1 e_s + S_r\tilde{\Phi}_r + \tau_r) - \tilde{\Phi}_r^T\left(S_r^T e_s - \frac{\hat{\Phi}_r - QB_c}{||\hat{\Phi}_r - QB_c||}\right) \\ &\le -e_s^T K_1 e_s + \tilde{\Phi}_r^T \frac{\hat{\Phi}_r - QB_c}{||\hat{\Phi}_r - QB_c||} - K_2\frac{e_s^T e_s}{||e_s||}.\end{aligned} \tag{34}$$

According to (22) and considering that $F\Phi_r = \Phi_r - QB_c$, $B_c = U_c\Phi_r$, (34) can be rewritten as follows:

$$\begin{aligned}\dot{L}_d = \; & -e_s^T K_1 e_s - (\hat{\Phi}_r - \Phi_r)^T \frac{\hat{\Phi}_r - QB_c}{||\hat{\Phi}_r - QB_c||} - K_2\frac{e_s^T e_s}{||e_s||} \\ \le \; & -(\hat{\Phi}_r - F\Phi_r - QB_c)^T \frac{\hat{\Phi}_r - QB_c}{||\hat{\Phi}_r - QB_c||} - K_2\frac{e_s^T e_s}{||e_s||} \\ \le \; & -(\hat{\Phi}_r - QB_c)^T \frac{\hat{\Phi}_r - QB_c}{||\hat{\Phi}_r - QB_c||} + ||F\Phi_r|| - K_2||e_s|| \\ \le \; & -||\hat{\Phi}_r - QB_c|| + ||F\Phi_r|| - K_2||e_s|| \\ \le \; & -||\Phi_r - QB_c + \hat{\Phi}_r - \Phi_r|| + ||F\Phi_r|| - K_2||e_s|| \\ \le \; & -||F\Phi_r - \tilde{\Phi}_r|| + ||F\Phi_r|| - K_2||e_s|| \\ \le \; & -||\tilde{\Phi}_r|| - K_2||e_s|| + 2||F\Phi_r|| \\ \le \; & -\mu_d\sqrt{L_d} + \rho_d\end{aligned} \tag{35}$$

where $\mu_d = \min\{\sqrt{2/\lambda_{\max}(\Gamma_d^{-1})}, K_2\sqrt{2/\lambda_{\max}(M)}\}$, $\rho_d = 2||F||||\Phi_r||$. Since F and Φ_r are bounded and $\lim_{t\to\infty} F = 0$, there exists a compact set $\Omega := \left\{\tilde{\Phi}_r | L_d(\tilde{\Phi}_r) \le (c/\mu_d)^2\right\}$ around zero, such that $\forall\tilde{\Phi}_r \notin \Omega$, $\dot{L}_d < 0$, where c is a small positive constant, which satisfies that $c > \gamma_d|\rho_d|$, $0 < \gamma_d < 1$. According to the result in [30], we can derive that the signal outside of Ω could enter this compact set within a finite time, and will remain inside the set for all future time. Hence, the parameter estimated errors are able to converge to a small compact set of their real values in the finite time. Besides, u_d could be chosen large by properly selecting Γ_d and K_2 and ρ_d will converge to zero when $t \to \infty$. This implies that the compact set Ω can be chosen small and will converge to zero when t is sufficiently large. The convergence rate could also be enhanced by choosing a larger gain Γ_d. ■

REFERENCES

[1] W. He, Z. Yan, C. Sun, and Y. Chen, "Adaptive neural network control of a flapping wing micro aerial vehicle with disturbance observer," *IEEE Trans. Cybern.*, vol. 47, no. 10, pp. 3452–3465, Oct. 2017.

[2] C. Yang, Y. Jiang, Z. Li, W. He, and C.-Y. Su, "Neural control of bimanual robots with guaranteed global stability and motion precision," *IEEE Trans. Ind. Informat.*, vol. 13, no. 3, pp. 1162–1171, Jun. 2017.

[3] C. Chen, Z. Liu, Y. Zhang, C. L. P. Chen, and S. Xie, "Actuator backlash compensation and accurate parameter estimation for active vibration isolation system," *IEEE Trans. Ind. Electron.*, vol. 63, no. 3, pp. 1643–1654, Mar. 2016.

[4] L. Cheng, Z.-G. Hou, M. Tan, and W.-J. Zhang, "Tracking control of a closed-chain five-bar robot with two degrees of freedom by integration of an approximation-based approach and mechanical design," *IEEE Trans. Syst., Man, Cybern., Part B, Cybern.*, vol. 42, no. 5, pp. 1470–1479, Oct. 2012.

[5] C. Yang, X. Wang, Z. Li, Y. Li, and C.-Y. Su, "Teleoperation control based on combination of wave variable and neural networks," *IEEE Trans. Syst., Man, Cybern., Syst.*, vol. 47, no. 8, pp. 2125–2136, Aug. 2017.

[6] C. F. Juang, Y. H. Chen, and Y. H. Jhan, "Wall-following control of a hexapod robot using a data-driven fuzzy controller learned through differential evolution," *IEEE Trans. Ind. Electron.*, vol. 62, no. 1, pp. 611–619, Jan. 2015.

[7] H. Davis and W. Book, "Torque control of a redundantly actuated passive manipulator," in *Proc. Amer. Control Conf.*, 1997, vol. 2, pp. 959–963.

[8] H. Cheng, Y.-K. Yiu, and Z. Li, "Dynamics and control of redundantly actuated parallel manipulators," *IEEE/ASME Trans. Mechatronics*, vol. 8, no. 4, pp. 483–491, Dec. 2003.

[9] C. Yang, G. Ganesh, S. Haddadin, S. Parusel, A. Albu-Schaeffer, and E. Burdet, "Human-like adaptation of force and impedance in stable and unstable interactions," *IEEE Trans. Robot.*, vol. 27, no. 5, pp. 918–930, Oct. 2011.

[10] Z. Liu, C. Chen, and Y. Zhang, "Decentralized robust fuzzy adaptive control of humanoid robot manipulation with unknown actuator backlash," *IEEE Trans. Fuzzy Syst.*, vol. 23, no. 3, pp. 605–616, Jun. 2015.

[11] Y. J. Liu and S. Tong, "Adaptive fuzzy identification and control for a class of nonlinear pure-feedback MIMO systems with unknown dead zones," *IEEE Trans. Fuzzy Syst.*, vol. 23, no. 5, pp. 1387–1398, Oct. 2015.

[12] C. Yang, K. Huang, H. Cheng, Y. Li, and C.-Y. Su, "Haptic identification by ELM-controlled uncertain manipulator," *IEEE Trans. Syst., Man, Cybern., Syst.*, vol. 47, no. 8, pp. 2398–2409, Aug. 2017.

[13] H. Kawasaki, T. Bito, and K. Kanzaki, "An efficient algorithm for the model-based adaptive control of robotic manipulators," *IEEE Trans. Robot. Autom.*, vol. 12, no. 3, pp. 496–501, Jun. 1996.

[14] C. G. Atkeson, C. H. An, and J. M. Hollerbach, "Estimation of inertial parameters of manipulator loads and links," *Int. J. Robot. Res.*, vol. 5, no. 3, pp. 101–119, 1986.

[15] W. He, W. Ge, Y. Li, Y.-J. Liu, C. Yang, and C. Sun, "Model identification and control design for a humanoid robot," *IEEE Trans. Syst., Man, Cybern., Syst.*, vol. 47, no. 1, pp. 45–57, Jan. 2017.

[16] R. Miranda-Colorado and J. Moreno-Valenzuela, "Experimental parameter identification of flexible joint robot manipulators," *Robotica*, vol. 36, pp. 313–332, Mar. 2018, doi: 10.1017/S0263574717000224.

[17] J. Moreno-Valenzuela and C. Aguilar-Avelar, *Motion Control of Underactuated Mechanical Systems*. Cham, Switzerland: Springer, 2018.

[18] J. Moreno-Valenzuela and C. Aguilar-Avelar, "Identification of underactuated mechanical systems," in *Motion Control of Underactuated Mechanical Systems*. New York, NY, USA: Springer, 2018, pp. 27–49.

[19] C. Aguilar-Avelar and J. Moreno-Valenzuela, "New feedback linearization-based control for arm trajectory tracking of the Furuta pendulum," *IEEE/ASME Trans. Mechatronics*, vol. 21, no. 2, pp. 638–648, Apr. 2016.

[20] C.-C. Cheah, C. Liu, and J. Slotine, "Adaptive Jacobian tracking control of robots with uncertainties in kinematic, dynamic and actuator models," *IEEE Trans. Automat. Control*, vol. 51, no. 6, pp. 1024–1029, Jun. 2006.

[21] C. C. Cheah, M. Hirano, S. Kawamura, and S. Arimoto, "Approximate Jacobian control for robots with uncertain kinematics and dynamics," *IEEE Trans. Robot. Autom.*, vol. 19, no. 4, pp. 692–702, Aug. 2003.

[22] L. Cheng, Z.-G. Hou, and M. Tan, "Adaptive neural network tracking control for manipulators with uncertain kinematics, dynamics and actuator model," *Automatica*, vol. 45, no. 10, pp. 2312–2318, 2009.

[23] J. Na, G. Herrmann, and K. Zhang, "Improving transient performance of adaptive control via a modified reference model and novel adaptation," *Int. J. Robust Nonlinear Control*, vol. 27, no. 8, pp. 1351–1372, 2017.

[24] P. M. Patre, W. Mackunis, M. Johnson, and W. E. Dixon, "Composite adaptive control for Euler–Lagrange systems with additive disturbances," *Automatica*, vol. 46, no. 1, pp. 140–147, 2010.
[25] Y. Lv, J. Na, Q. Yang, X. Wu, and Y. Guo, "Online adaptive optimal control for continuous-time nonlinear systems with completely unknown dynamics," *Int. J. Control*, vol. 89, no. 1, pp. 99–112, 2016.
[26] J. Na, M. N. Mahyuddin, G. Herrmann, X. Ren, and P. Barber, "Robust adaptive finite-time parameter estimation and control for robotic systems," *Int. J. Robust Nonlinear Control*, vol. 25, no. 16, pp. 3045–3071, 2015.
[27] M. Gautier, "Numerical calculation of the base inertial parameters of robots," *J. Robot. Syst.*, vol. 8, no. 4, pp. 485–506, 2007.
[28] Y. Pan, M. J. Er, D. Huang, and Q. Wang, "Adaptive fuzzy control with guaranteed convergence of optimal approximation error," *IEEE Trans. Fuzzy Syst.*, vol. 19, no. 5, pp. 807–818, Oct. 2011.
[29] K. Radkhah, D. Kulic, and E. Croft, "Dynamic parameter identification for the CRS a460 robot," in *Proc. Int. Conf. Intell. Robots Syst.*, 2007, pp. 3842–3847.
[30] V. I. Utkin, *Sliding Modes in Control and Optimization*. New York, NY, USA: Springer, 2013.

Chenguang Yang (M'10–SM'16) received the B.Eng. degree in measurement and control from Northwestern Polytechnical University, Xi'an, China, in 2005, and the Ph.D. degree in control engineering from the National University of Singapore, Singapore, in 2010.

He received Postdoctoral training at Imperial College London, UK. His research interests lie in robotics and automation.

Prof. Yang was awarded Marie Curie International Incoming Fellowship, Best Paper Award of the IEEE Transactions on Robotics and Best Paper Awards from numerous international conferences.

Yiming Jiang received the B.S. degree in automation from Hunan University, Changsha, China, in 2011, the M.S. degree in control theory and engineering from the School of Automation, Guangdong University of Technology, Guangzhou, China, in 2015, and is currently working toward the Ph.D. degree in pattern recognition and intelligent systems with the School of Control Science and Engineering, South China University of Technology, Guangzhou, China.

His research interests include robotics, intelligent control, human–robot interaction, etc.

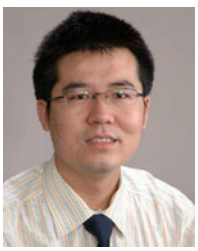

Wei He (M'12–SM'16) received the B.Eng. and M.Eng. degrees in control engineering from the College of Automation Science and Engineering, South China University of Technology, Guangzhou, China, in 2006 and 2008, respectively, and the Ph.D. degree in control engineering from the Department of Electrical and Computer Engineering, National University of Singapore, Singapore, in 2011.

He is currently a Full Professor with the School of Automation and Electrical Engineering, University of Science and Technology Beijing, Beijing, China. He has coauthored 2 book published in Springer and authored or coauthored more than 100 international journal and conference papers. His current research interests include robotics, distributed parameter systems, and intelligent control systems.

He was the recipient of a Newton Advanced Fellowship from the Royal Society, U.K., the IEEE SMC Society Andrew P. Sage Best Transactions Paper Award in 2017. He is the Chair of IEEE SMC Society Beijing Capital Region Chapter. He is an Associate Editor of the IEEE TRANSACTIONS ON NEURAL NETWORKS AND LEARNING SYSTEMS, the IEEE TRANSACTIONS ON SYSTEMS, MAN, AND CYBERNETICS: SYSTEMS, and IEEE ACCESS, and an Editor of the IEEE/CAA JOURNAL OF AUTOMATICA SINICA, *Neurocomputing*, and *Journal of Intelligent and Robotic Systems*. He is the member of the IFAC TC on Distributed Parameter Systems, IFAC TC on Computational Intelligence in Control, and IEEE CSS TC on Distributed Parameter Systems.

Jing Na (M'15) received the B.S. degree in automation and Ph.D. degree in dynamics and control from the School of Automation, Beijing Institute of Technology, Beijing, China, in 2004 and 2010, respectively.

From 2011 to 2013, he was a Monaco/ITER Postdoctoral Fellow with the ITER Organization Saint-Paul-lz-Durance, France. From 2015 to 2017, he was a Marie Curie Intra-European Fellow with the Department of Mechanical Engineering, University of Bristol, Bristol, U.K. Since 2010, he has been with the Faculty of Mechanical and Electrical Engineering, Kunming University of Science and Technology, Kunming, China, where he became a Professor in 2013. His current research interests include intelligent control, adaptive parameter estimation, nonlinear control, and their applications.

Prof. Na is an Associate Editor for *Neurocomputing*. He was the recipient of the Best Application Paper Award of the third IFAC International Conference on Intelligent Control and Automation Science (IFAC ICONS 2013), and 2017 Hsue-shen Tsien Paper Award.

Zhijun Li (M'07–SM'09) received the Ph.D. degree in mechatronics from Shanghai Jiao Tong University, Shanghai, China, in 2002.

Since 2012, he has been a Professor with the College of Automation Science and Engineering, South China University of Technology, Guangzhou, China. His current research interests include service robotics, teleoperation systems, nonlinear control, neural network optimization, etc.

Dr. Li is an Editor-at-Large for *the Journal of Intelligent and Robotic Systems*, an Associate Editor for the IEEE TRANSACTIONS ON NEURAL NETWORKS AND LEARNING SYSTEMS, IEEE TRANSACTIONS ON SYSTEMS, MAN, AND CYBERNETICS: SYSTEMS, and IEEE TRANSACTIONS ON AUTOMATION SCIENCE AND ENGINEERING. He has been the General Chair for 2016 IEEE Conference on Advanced Robotics and Mechatronics, Macau, China.

Bin Xu received the B.S. degree in measurement and control from Northwestern Polytechnical University, Xi'an, China, in 2006, and the Ph.D. degree in computer science from Tsinghua University, Beijing, China, in 2012.

He is currently a Professor with the School of Automation, Northwestern Polytechnical University. His research interests include intelligent control and adaptive control with application to flight dynamics.

Dr. Xu is an Associate Editor for *Neurocomputing*, *International Journal of Advanced Robotic Systems*, *Chinese Journal of Aeronautics,* and *Science China Information Sciences*.